Molecular Phylogenetics and Evolution 134 (2019) 269–281

Contents lists available at ScienceDirect

Molecular Phylogenetics and Evolution

journal homepage: www.elsevier.com/locate/ympev

Unravelling population processes over the Late Pleistocene driving contemporary genetic divergence in Palearctic buzzards

Michael J. Jowers[a,*], Santiago Sánchez-Ramírez[b], Susana Lopes[a], Igor Karyakin[c], Valery Dombrovski[d], Abdeljebbar Qninba[e], Thijs Valkenburg[f], Nuno Onofre[g], Nuno Ferrand[a,h,i], Pedro Beja[a,j], Luís Palma[a,1], Raquel Godinho[a,h,i,1]

[a] CIBIO/InBIO, Centro de Investigação em Biodiversidade e Recursos Genéticos, Universidade do Porto. Campus de Vairão, 4485-661 Vairão, Portugal
[b] Department of Ecology and Evolutionary Biology, University of Toronto, 25 Willcocks, Toronto, Ontario M5S 3B2, Canada
[c] Sibecocenter, LLC, POBox 547, 630090 Novosibirsk, Russia
[d] Laboratory of Molecular Zoology, National Academy of Sciences of Belarus, Academicheskaya 27, 220072 Minsk, Belarus
[e] Mohammed V University in Rabat, Scientific Institut, Geo-Biodiversity and Natural Heritage Laboratory, Avenue Ibn Battouta, BP 709, 10090 Agdal, Rabat, Morocco
[f] RIAS, Wildlife Rehabilitation and Research Centre, Olhão, Portugal
[g] National Agrarian and Veterinarian Research Institute, I.P., Quinta do Marquês, 2780-159 Oeiras, Portugal
[h] Departamento de Biologia, Faculdade de Ciências, Universidade do Porto, Rua do Campo Alegre s/n, 4169-007 Porto, Portugal
[i] Department of Zoology, University of Johannesburg, PO Box 534, Auckland Park 2006, South Africa
[j] CIBIO/InBIO, Centro de Investigação em Biodiversidade e Recursos Genéticos, Instituto Superior de Agronomia, Universidade de Lisboa, Lisboa, Portugal

ARTICLE INFO

Keywords:
Buzzards
Palearctic
Late Pleistocene
Genetic divergence
Phylogeography

ABSTRACT

Population range expansions and contractions as a response to climate and habitat change throughout the Quaternary are known to have contributed to complex phylogenetic and population genetic events. Speciation patterns and processes in Palearctic buzzards (genus *Buteo*) are a long-standing example of morphological and genetic data incongruence, attributed to panmixia, habitat range shifts, contact zones, and climate change. Here we assess the systematics, phylogeography and population genetic structure of three nominal species of Palearctic buzzards, *Buteo buteo* (including *B. b. vulpinus*), *B. rufinus* (including *B. r. cirtensis*) and *B. hemilasius*. Phylogenetic analyses inferred from mitochondrial data recover *B. hemilasius* as sister to the sister clades *B. r. rufinus* and *B. buteo* complex (*B. b. buteo*, *B. b. vulpinus*, but also including *B. r. cirtensis*). In contrast, we find an unresolved genetic delimitation inferred from four nuclear loci, suggesting an ancestral genetic pool for all species. Time-trees suggest population contractions and expansions throughout the Pleistocene, which likely reflect habitat change and contrasting ecological niche requirements between species. Microsatellite-based extended Bayesian skyline plots reveal relatively constant population sizes for *B. hemilasius*, *B. r. rufinus*, and *B. b. vulpinus*, in contrast to a dramatic population expansion in *B. r. cirtensis* within the last 3 kya. Overall, our study illustrates how complex population processes over the Late Pleistocene have shaped the patterns of genetic divergence in Palearctic buzzards, due to the joint effects of shared ancestral polymorphisms, population expansions and contractions, with hybridization at contact zones leading to admixture and introgression.

1. Introduction

Species are the fundamental units to assess biogeography, ecology and evolutionary biology as a whole (Barraclough and Nee, 2001; Coyne and Orr, 2004). Consequently, analysis of species biodiversity is paramount to understanding evolutionary processes involved in speciation with pivotal implications for conservation (Sites and Marshall, 2003). Today, species are understood as separate evolving lineages (de Queiroz, 2007) in which subpopulations form distinct evolutionary 'paths' in the tree of life. However, establishing which operational criteria should be used to assign individuals to species remains largely problematic and debatable (Aldhebiani, 2017). Multidisciplinary taxonomy through the integration of morphology and genetic data remains complex, often resulting in taxonomical incongruence and discordance between species relationships, especially so, in rapid and recent radiations (Wagner et al., 2012) and in taxa with weak species boundaries

* Corresponding author.
E-mail address: Michaeljowers@hotmail.com (M.J. Jowers).
[1] These two authors contributed equally.

https://doi.org/10.1016/j.ympev.2019.02.004
Received 21 September 2018; Received in revised form 1 February 2019; Accepted 4 February 2019
Available online 11 February 2019

(Willis et al., 2012). The employment of morphological characters can often lead to misleading phylogenetic interpretation through disruptive selection and low character variability. In particular, this is largely evident at the early stages of speciation or when gene tree/species tree discordance occurs through introgressive hybridization or incomplete lineage sorting (Nosil et al., 2009). Yet, delimiting species units is generally more often than not based on phenetic variability where geographical variation in phenotypes is commonly linked to speciation processes (Endler, 1977).

Palearctic buzzards (genus *Buteo*) are medium size birds of prey with similar predatory habits but different habitats and movement patterns, which exhibit a variable degree of chromatic polymorphism and are a long-standing example of morphological and genetic data incongruence to assess taxonomical status (Kruckenhauser et al., 2004). Despite the fact that the Common buzzard (*B. buteo*) is the most common raptor species in most parts of its Eurasian range (Ferguson-Lees and Christie, 2001), its taxonomy and the relationship between subspecies and closely related species remains obscure (Mindell et al., 1998; Wink et al., 1998). Taxonomic confusions occur in all three Common buzzard groups, the *buteo* group (Western/Central Europe including Atlantic and Mediterranean islands), the *vulpinus* group (Northern/Eastern Europe eastwards across Siberia) and the *japonicus* group (East Siberia, Japan, China, India and Indochina*)*. Thus, from an evolutionary perspective, the lack of clearly defined genetic and morphological entities throughout the wide range of the *B. buteo* species complex seems both surprising and quite possibly unique among raptors. Reasons for the occasional taxonomical incongruence within and between groups may be due to: (i) a very recent radiation, accounting for the accumulation of insufficient genetic divergence between forms, (ii) the existence of contact zones between the breeding areas or the movement of dispersers among geographically non-overlapping ranges, and (iii) ancestral polymorphism derived from the most common recent ancestral population still present throughout the populations. Several molecular studies, mostly based on mitochondrial DNA, have addressed the unresolved systematics of some of the *B. buteo* and *B. rufinus* subspecies but have failed to determine the relationship between the attributed species and subspecies (Mindell et al., 1998; Wink et al., 1998; Haring et al., 1999; Riesing et al., 2003; Lerner et al., 2008; Do Amaral et al., 2009). Kruckenhauser et al., (2004) argue that the taxonomical complexity in West Palearctic buzzard taxa is a consequence of low genetic differentiation derived from extensive gene flow within the *buteo-vulpinus-rufinus-oreophilus* complex. They suggest treating *B. buteo* as a superspecies (Mayr, 1963; Haffer, 1997; Helbig, 2000) comprising three allospecies *B. [buteo] buteo* (with 9 subspecies), *B. [b.] rufinus* (with 2 subspecies including *B. r. cirtensis*) and *B. [b.] oreophilus*.

Palearctic buzzards are thought to have evolved within a short timeframe, possibly through the reduction of ranges during ice ages. Differentiated gene pools in *Buteo* species have been attributed to expansions from their ranges during the interglacial periods, resulting in poorly differentiated entities (Haring et al., 1999). In fact, the Pleistocene climatic conditions played a central role in shaping species diversity across the globe contributing to speciation events (Hewitt, 1996, 2000; Avise, 1997; Avise et al., 1998; Knowles, 2001; Veith et al., 2003). A recent study on whole-genome sequences of 38 avian species revealed that more than half showed dramatic historical population size (N_e) declines just at the beginning of the Last Glacial Maximum (LGM) (20 kya BP, Prentice et al., 2000; 33–26.5 kya; Clark et al., 2009). The authors concluded that population expansions and contractions were common in avian species in the Quaternary (Nadachowska-Brzyska et al., 2016). Recently, the LGM in Europe resulted in speciation patterns following the isolation of populations on southern peninsulas used as refugia from colder and drier conditions (Taberlet et al., 1998; Morales-Barbero et al., 2017). Thus, it is apparent that the LGM contributed significantly to the intraspecific divergence of populations through contractions and expansions from refugia but did not trigger speciation processes (Pulgarín-R and Burg, 2012). Genetic divergence ultimately contributing to speciation processes is more likely in allopatric populations that have been separated by geographical barriers (Hewitt, 1996). Hence, it is reasonable to assume that species with high dispersal capacity (potential to settle far from birthplace), such as raptors, would show less genetic subdivision due to (i) sympatry at breeding contact zones through gene flow during early speciation stages and (ii) through hybridization and gene introgression.

Hybridization and introgression are well known to occur in many bird species contact zones and variable offspring have been documented in about 10% of all studied bird species (Helbig, 2000; Randler, 2004), but to a lesser extent in birds of prey (Fefelov, 2001; Löhmus and Väli, 2001; Helbig et al., 2005; Nittinger et al., 2007). Buzzards are well known to hybridize in the wild (McCarthy, 2006). *B. r. rufinus* hybridization with *B. buteo* has been documented in Hungary (Dudás et al., 1999), with *B. hemilasius* in central Asia (Pfänder and Schmigalew, 2001) and with *B. b. vulpinus* in India (McCarthy, 2006). Hybridization between *B. r. cirtensis* and *B. buteo* has also been documented in Tunisia (Corso, 2009) and in the Straits of Gibraltar in recent years (Elorriaga and Muñoz, 2013). However, hybridization raises questions about how the different parent morphs may have an effect on assortative mating through chick imprinting on maternal genotypes (Krüger et al., 2001). Furthermore, highly variable colour plumage within species and similarity of colours between species throughout temporary overlapping home ranges (BirdLife International, 2019) has challenged taxonomic arrangements. For example, the chromatic polymorphic ranges of *Buteo b. buteo* go from uniformly blackish-brown to mainly white, but most are typically dark brown. *Buteo b. vulpinus* is slightly smaller, distinctly polymorphic with three main morphs, grey-brown, dark, and rufous of which the latter is the commonest. *Buteo r. rufinus* is a large-sized buzzard, polymorphic from creamy and rufous to almost blackish coloured. *Buteo r. cirtensis* is much smaller, polymorphic and individually variable. *Buteo hemilasius* is a large-sized buzzard, dimorphic with pale and dark morphs and partially feathered tarsi. *B. b. buteo* is sedentary to short-distance migratory, wintering mainly in southern Europe and North Africa. *B. b. vulpinus* is highly migratory, wintering across eastern and southern Africa, and reaching Iran and India to the East. *B. rufinus* is fully migratory in North and East of its range, partly resident in the South, wintering from the eastern Mediterranean, Middle East and Arabia to the north of the Indian Subcontinent. *B. r cirtensis* is presumably largely sedentary and dispersive while *B. hemilasius* movements vary from sedentary, nomadic and partially migratory in lower ground to fully migratory in the north and high uplands, wintering from southern Kazakhstan and southern Himalayas to eastern China (Ferguson-Lees and Christie, 2001).

In Common Buzzards (*Buteo buteo*), many aspects of behaviour, physiology, and life history are morph dependent, including mate choice and aggression (Krüger et al., 2001; Boerner and Krüger, 2008), habitat choice (Krüger, 2002), blood parasite prevalence and infection intensity and ectoparasite infestation (Chakarov et al., 2008). Plumage morphs in Common Buzzards strongly differ in lifetime reproductive success (LRS), a key component of fitness (Krüger et al., 2001), with intermediate melanised morphs having the highest LRS. Thus, speciation patterns and processes in Old World Buzzards may therefore be more intricate than expected, with ecological and non-ecological processes both playing a part in selection of morphs in contact zones. Thus, non-ecological speciation driving morphotypes in contact zones through assortative mating and random genetic drift through population fluctuations is opposed to ecological speciation. Under ecological speciation, environmental differences and local adaptation result in reproductive isolation (Rundle and Nosil, 2004). Recently established populations of buzzards with little adaptation to local environments and lack of geographical barriers suggest that complete reproductive isolation is not expected in neighbour populations, resulting in mixed ancestral polymorphisms.

In this study, we used molecular analyses to assess population structure and phylogeography of three recognized nominal species of

Palearctic buzzards, *Buteo buteo* (including *B. b. vulpinus*), *Buteo rufinus* (including *B. r. cirtensis*) and *Buteo hemilasius*. With mitochondrial and nuclear data, we (i) examined historical demographic patterns to understand how recent past climatic changes may have structured the species populations and establish the time of major population expansions throughout the distribution range, (ii) assessed present gene flow, and (iii) established the genetic identity of two controversial forms, *B. r. cirtensis* and *B. b. vulpinus*. To such purpose, we simultaneously employed for the first time in an Old World Buzzard molecular study mitochondrial and nuclear sequences, and microsatellite data. We collected samples from across all three nominal species breeding ranges, *B. buteo* from Portugal to Southern Siberia, *B. r. rufinus* from Bulgaria to Kazakhstan and Uzbekistan, *B. r. cirtensis* from Morocco to Tunisia and *B. hemilasius* from the Altai to Dauria (Transbaikal) in the Russian Federation. Thus, herein we enhance on the historical and the present demographic events that have shaped and continue to shape the populations of Palearctic buzzards.

2. Material and methods

2.1. Sampling and outgroup data

Samples were primarily obtained from moult feathers collected in the field and stored in zip-lock plastic bags at −20 °C. Some feather tips and fresh tissue samples were preserved in absolute ethanol. Blood samples were extracted from birds held at rehabilitation centres, and dry toe pads or other tissues were taken from museum specimens. Samples from Germany were obtained as isolated DNA dissolved in water. We collected a total of 298 samples and obtained DNA amplification from 245 of them. However, amplification of all molecular markers with complete confidence of origin (locality) was ultimately available from 181 samples (Supplementary material SM Table 1), which were used for the phylogeographic and demographic analyses. A total of 205 and 222 samples were sequenced and genotyped, respectively. These samples spread across the extant Eurasian breeding range of *B. buteo* (including *B. b. vulpinus*), *B. rufinus* (including *B. r. cirtensis*) and *B. hemilasius*. As outgroup, we used two New World species of *Buteo* with mitochondrial sequences retrieved from GenBank: *B. swainsoni* (AY213028 and GQ264806, New Mexico, USA) and *B. galapagoensis* (AY213026, GQ264783, Galapagos Islands).

2.2. DNA extraction, sequencing and genotyping

Whole genomic DNA was extracted using the DNeasy Blood & Tissue kit (QIAGEN, Hilden, Germany) following the manufacturers' instructions or with the standard high-salt protocol of Sambrook et al. (1989). The targeted mitochondrial gene fragments were Cytochrome *b* (cyt *b*), *NADH dehydrogenase* 6 (Nd6) and Pseudo-control region (ψCR), and the nuclear loci were *recombination activating gene 1* (RAG-1), *Parkinson disease associated gene* 7 intron2 (PARK7), *muscle-specific tyrosine kinase receptor* intron 3 (MUSK) and *fibrinogen* intron 5 (FIB) (see SM Table 2 for primers). Individual multilocus genotypes were screened for 32 autosomal microsatellite loci previously developed for *B. buteo* (Johnson et al., 2005) and *B. swainsoni* (Hull et al., 2007) using four multiplex reactions (see SM Table 2 for loci and PCR conditions). We followed a fluorescent labelling protocol (Blacket et al., 2012) across PCR amplifications, and included always a negative control to monitor contamination. Amplicons were separated by size in an ABI3130xl genetic analyser. Allele sizes were scored against the GeneScan500 LIZ size standard using GENEMAPPER 4.0 (Applied Biosystems) and checked manually by two researchers. The accuracy of the results was measured through re-amplification of 15% random selected samples for each locus (Bonin et al., 2004) resulting in complete concordance among replicates. Ten loci exhibiting low amplification rates were removed from analysis. The presence of null alleles was checked in MICROCHECKER 2.2.3 (van Oosterhout et al., 2004).

2.3. mtDNA and nuDNA genetic diversity

Polymorphic positions corresponding to heterozygous individuals in nuclear loci were coded with IUPAC ambiguity codes and all sequences were phased using DnaSP v.5.10.1 (Librado and Rozas, 2009). Six markers, including two mitochondrial (mtDNA) fragments and four nuclear (nuDNA) gene fragments were analysed; mtDNA: 750 bp of cytochrome *b* (cyt *b*) and the fragment (648 bp) comprising 293 bp of the pseudo-control region (ΨCR), 74 bp of the TRNA-Glu and 281 bp of the ND6 (cyt *b* + ΨCR + ND6 + TrnaGLU, total 1398 bp), nuDNA: a 462 bp fragment of RAG-1, 667 bp of PARK7, 532 bp of MUSK, and 911 bp of FIB. Sequences were checked visually, edited and aligned using the program Sequencer v.4.9 (Applied Biosystems) and Seaview v.4.2.12 (Gouy et al., 2010). All sequences were edited and aligned independently by two researchers to assess possible incongruence in sequence editing. All sequences generated for this study were deposited in Genbank (SM Table 1). All known haplotypes were incorporated for subsequent haplotype inference. We accepted haplotypes with a minimum probability of 0.9. We performed phylogenetic analyses in MrBayes v3.2.1 (Ronquist and Huelsenbeck, 2003). Full alignments were collapsed into haplotypes using the online tool Fabox (Villesen, 2007) (SM Table 3). For the mtDNA dataset, we used PartitionFinder v1.1.1 (Lanfear et al., 2012) to choose the optimal partitioning strategy. The best partition scheme was obtained for five partitions, corresponding to first position in cyt *b* and the fragment containing the tRNA; second positions in cyt *b*; third positions in cyt *b*; fourth partition with the ΨCR and ND6 second position and; fifth partition with ND6 first and third codon positions. The rate of the ΨCR has been estimated to be much faster evolving than the CR (Haring et al., 1999). However, the mutation rate of the avian control region is uncertain (Hansson et al., 2008). Thus, to such purpose we calculated the *p*-distances of the cyt *b*, Nd6 and ΨCR separately.

2.4. Sequencing data: Phylogenetic and biogeographic analyses

Bayesian inference (BI) (MrBayes v3.2.1; Ronquist and Huelsenbeck, 2003) of haplotypes with outgroups (see methods; sampling) were used with default priors and Markov chain settings, and with random starting trees. Each run consisted of four chains of 20,000,000 generations, sampled every 2000 generations. A plateau was reached after few generations with 20% of the trees discarded as burn-in. Phylogenetic relationships among haplotypes for each locus were estimated using a Maximum Likelihood (ML) approach with outgroups, as implemented in the software RAxML v7.0.4 (Silvestro and Michalak, 2012), under the best partition scheme and GTR model. All analyses were performed through the CIPRES platform (Miller et al., 2010). Branch-specific rates and lengths were visualized with FigTree 1.4.2 (Rambaut, 2014). Networks were built on Haploviewer (Salzburger et al., 2011) under the best tree topology as inferred in RAxML. We performed statistical coalescent and phylogeographic analyses using BEAST v1.8.2 (Drummond et al., 2012; http://beast.bio.ed.ac.uk). First we specified separate nucleotide substitution and molecular clock models; HKY (cyt *b*), HYK (ND6) and HKY + I (ΨCR) and strict clock for each gene fragment, respectively. In order to time-calibrate the population tree, we fixed the mutation rate in the cyt *b* to 2.5×10^{-8} substitutions/site/year and the ND6 and ΨCR rate estimated from the prior. This cyt *b* rate is similar to the one in Galliforms (5.04%) and in Galapagos mockingbirds (genus *Nesomimus*; 5.52%) (Dovretsky, 2003). Similar estimates have been used in raptors on diverse mitochondrial markers, (i.e. 4%) (Garcia et al., 2011; Nabholz et al., 2009; Monti et al., 2015) and other avian species (Peck and Congdon, 2004; Garcia et al., 2008; Arbogast et al., 2016). In addition to the population tree, we co-estimated the dispersal history using a discrete phylogeographic (ancestral state reconstruction) model also implemented in BEAST (Lemey et al., 2009). Given that our geographic sampling of populations is uneven and our state-space is low, we chose

a symmetric continuous time rate matrix. As priors for the rates, we selected the approximate reference (CTMC) prior (Ferreira and Suchard, 2008). The discrete BI analyses were run for 300 million generations and sampling every 30,000 generations. Secondly, we estimated the diffusion of all three *Buteo* species mitochondrial gene fragments partitions through time using the continuous Bayesian phylogeographic approach (Lemey et al., 2010). This approach estimates population range changes through time and ancestral populations' locations. We used the Cauchy RRW (SM Table 4) model with all individuals assigned to GPS coordinates. A random "jitter" was added to each GPS coordinate with a window size of 0.5. We applied a fixed clock rate to the cyt *b* data set and estimated from the prior for the ND6 and ΨCR. We used marginal likelihood estimations (MLE) and Bayes factors (BF) to select for the continuous trait model. MLE were calculated through path sampling (PS) and stepping stone (SS) analyses in BEAST (Baele et al., 2012). We tested for Brownian, Cauchy, Gamma and Lognormal RRW models under the strict and relaxed lognormal models running 300 million generations with sampling every 30,000 generations. For all the models tested, MLE analyses were run for 50 path steps and 100,000 generations with each step. The BF were calculated as two times the difference in MLE between different models, and the significance was determined if the BF value was > 10 (Kass and Raftery, 1995). SPREAD (Bielejec et al., 2011) was used to compute spatial continuous space MCC trees and viewed in Google Earth (http://earth.google.com). Thirdly, we inferred changes in effective population sizes through time for all three nominal species independently (*B. buteo*, *B. rufinus* and *B. hemilasius*) using a Bayesian Skyline Plot (BSP) model (Drummond et al., 2005) with strict clock for the cyt *b* data and same priors as above. Independent runs were evaluated for convergence and mixing by observing and comparing traces of each parameter in Tracer v1.6 (Rambaut et al., 2013). We considered effective sampling size (ESS) values > 200 to be good indicators of parameter mixing. The first 10% and 25% states of the Discrete, BSP and Continuous Bayesian phylogenies (n = 169) were discarded as burn-in, respectively. The resulting trees were summarized using TreeAnnotator v1.8.2 (Rambaut and Drummond, 2015), where a maximum clade-credibility (MCC) tree with mean values was generated under heights = ca (Heled and Bouckaert, 2013). In the case of BSP, log and tree files were uploaded into Tracer, in which the plot was generated.

2.5. Sequencing data: Demographic analyses

To examine whether the species showed any sign of historical population expansion, we estimated Tajima's D (Tajima, 1989), Fu's Fs (Fu, 1997), Ramos-Onsins and Rozas' R^2 (Ramos-Onsins and Rozas, 2002) and a mismatch distribution analysis (Rogers and Harpending, 1992) for every subspecies using ARLEQUIN 3.0 (Excoffier et al., 2005). Negative values of Tajima's D can be interpreted as evidence of population expansions (Fu, 1997), and negative values of Fs indicate an excess of recent mutations and reject population stasis. A diagram of frequencies of pairwise genetic differences was drawn using DnaSP v.5.0 (Librado and Rozas, 2009). A thousand bootstrap replicates were used to generate an expected distribution using a model of sudden demographic expansion (Excoffier et al., 2005). The sum of squared deviation (SSD) and the raggedness index were also calculated. These measures quantify the smoothness of the observed mismatch distribution. Mismatch distribution is usually multimodal in samples drawn from populations at demographic equilibrium, but is usually unimodal in populations following recent population demographic and range expansion (Slatkin and Hudson, 1991; Rogers and Harpending, 1992; Ray et al., 2003). Small raggedness values are typical of an expanding population whereas higher values are observed among stationary or bottlenecked populations (Harpending et al., 1993).

The historical demography of *B. buteo*, *B. r. rufinus* and *B. hemilasius* was also estimated based on the mitochondrial dataset using Bayesian Skyline Plots (BSP; Drummond et al., 2005) implemented in BEAST 1.8.2. BSP analyses were performed on each species or subspecies separately for which enough sampling was available. Analyses were run according to the best BIC model suggested in jModelTest (Posada, 2008). BSP analyses were thus conducted using a strict molecular clock with a substitution rate of our estimated cyt *b* to 2.5×10^{-8} substitutions/site/year and the ND6 and ΨCR rate estimated from the prior. Analyses were run for 100 million generations, sampled every 10,000. A 10% was discarded as burn-in. We used Tracer 1.6 to draw the BSP.

The extent of geographical structuring of genetic variation between groupings from all sampled areas was evaluated by Fst and Φst statistics, testing for significance variance in the distribution of mitochondrial and microsatellite data between groups of populations, populations and individuals using the analysis of molecular variance (AMOVA) in ARLEQUIN 3.0 (Excoffier et al., 2005). The significance of variance components and F-statistics were assessed by permutations (10,000) of the data sets.

2.6. Microsatellite genetic diversity and differentiation

Multilocus genotypes were used to estimate microsatellite diversity in ARLEQUIN 3.5 (Excoffier and Lischer, 2010) based on observed (Ho) and expected (He) heterozygosity and inbreeding coefficient (FIS) for each group defined previously with mitochondrial and nuclear sequencing. ARLEQUIN was also used to calculate departures from expectations under Hardy–Weinberg equilibrium (HWE) following Guo and Thompson (1992), and to test linkage disequilibrium between loci. Statistical significance was adjusted using Bonferroni correction for multiple testing (Rice, 1989). The same software was used to estimate pairwise differentiation among the different groups using FST and RST statistics. Allelic richness (AR) was estimated in FSTAT 2.9.3.2 (Goudet, 1995) using a rarefaction procedure to compensate for differences in sample size.

Microsatellite genotypes were also analysed using the Bayesian clustering software STRUCTURE 2.3.4 (Pritchard et al., 2000; Falush et al., 2003) to test for the number of populations (K) independent of spatial sampling. Analyses were performed using the admixture model with correlated allele frequencies in ten independent runs from K = 1 to K = 10, with 10^6 MCMC iterations after an initial burn-in of 10^5 iterations. The most likely number of populations present in the dataset were inferred after plotting the mean likelihood L(K) of STRUCTURE runs and the ΔK method of Evanno et al. (2005) (SM Fig. 1) and outputs were inspected in Harvest (Earl, 2011). The assignment values for each individual for the most likely number of populations were plotted in a map using QGIS 2.14 (QGIS Development Team, 2014). Population structure was additionally tested by model-independent multivariate analyses, using a discriminant analyses of principal components (DAPC) performed in ADEGENET v1.2.8 in R (Jombart et al., 2010).

2.7. Microsatellite Extended Bayesian Skyline Plots (EBSP)

We used microsatellite data to estimate changes in effective population size through time using the Extended Bayesian Skyline Plot (EBSP) model as implemented in the BEAST v1.8.4 package (Drummond et al., 2012). A custom R script (excel2msatLen.R) was used to convert allelic data scored as microsatellite length to the difference in repeat counts between alleles. For each locus *i*, the length in bp of all alleles *j* was stored in a vector *A*. Then, the difference in the number of repeats between alleles was calculated as:

$$R_j = \frac{j - minA_{j\ldots n}}{m_i} + 1$$

where *m* is the size of the motive (e.g. di-, tri-, tetranucleotide) for a particular locus. A second R script (excel2msatBEAST.R) was used to convert the matrix to a BEAST acceptable format. The site model for different loci was linked, but the clock models and partition trees were not. For the substitution model, we specified equal rates, linear

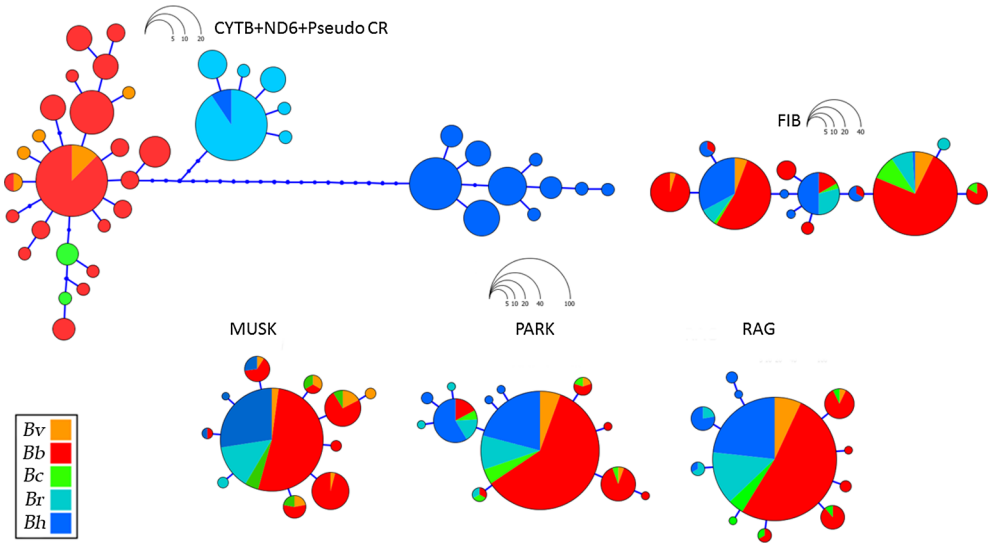

Fig. 1. ML networks. Combined mtDNA (cyt *b* + ND6 + ΨCR, n = 181, bp = 1324), nuDNA: 462 bp fragment of the reactivation combining gene (RAG-1, n = 290 diphased), 667 bp of PARK7 intron2 (n = 278 diphased), 532 bp of me MUSK intron 3 (n = 268 diphased), and 911 bp of the fibrinogen intron 5 (FIB n = 234 diphased).

mutation bias and a two-phase model. For the strict clock model, we used a mutation rate of 1.16×10^{-4} based on a chicken pedigree (Hillel et al., 2003). Preliminary runs with the Lesser Kestrel (*Falco naumanni*) mutation rate 2.96×10^{-3} (Ortego et al., 2008) resulted in too recent demographic patterns, which were biologically unrealistic. Although we consider the chicken estimate to be plausible, we also discuss our results in the light of a different choice of mutation rate (see Discussion). A linear model was specified for the EBSP coalescent tree prior, and ploidy was set to autosomal nuclear. Default priors were used for model parameters and statistics, except for the demographic population mean where we used a lognormal distribution (mean = 50000, sd = 1, offset = 0, with mean in real space), based on the results of an exploratory BEAST run with a constant size tree prior using a combination of samples. As suggested by other BEAST users, we increased the weight of the operator "randomWalkIntegerOperator" to 100 for all loci. XML files for each subspecies were run for 2×10^9 generations (about 4 months of CPU time) in order to achieve decent mixing for most parameters (ESS > 200). The MCMC chain was visited every 200,000th state for a total of 10,000 sampled states. Log files were checked in Tracer v1.6 (Rambaut et al., 2013) and the resulting CSV files were plotted in R using the script RplotEBS.R. All scripts are available at https://github.com/santiagosnchez. Five taxa (though see results) were analysed; *B. b. buteo*, *B. b. vulpinus*, *B. r. cirtensis*, *B. r. rufinus*, *B. hemilasius*.

Because of the taxonomic complexity, debatable systematics, and the nature of the study, which focused on population genetics rather than phylogenetics, and for practical reasons of simplicity and clarity of the text we hereafter refer to the studied taxa solely by their subspecific name whenever enough for recognizing which taxon is concerned, unless otherwise justified.

3. Results

3.1. Sequencing data

The combined mitochondrial DNA alignment employed for the Bayesian analyses comprised a total of 181 sequences for all targeted mitochondrial fragments (cyt *b*, Nd6 and ΨCR, 1324 bp) and were included in the final analyses. Because of the lack of genetic divergence of the TRNA-GLU (74 pb) in all samples (n = 181) it was excluded from all analyses. The nuclear phased markers resulted in a 462 bp fragment of RAG-1 (n = 290 diphased), 667 bp of PARK7 (n = 278 diphased), 532 bp of MUSK (n = 268 diphased), and 911 bp of FIB (n = 234 diphased). Three individuals from Tuva (Russia) identified morphologically as *hemilasius* (BT120, BT124, BT138) showed mitochondrial introgression within the *rufinus* clade, and so they were excluded from the demographic analyses.

3.2. Mutation rates and divergence

The concatenated mitochondrial sequences (1324 bp) of the 181 individuals were collapsed to 40 haplotypes (SM Table 3). The ΨCR was 3.2 times faster than the cyt *b* and 3.1 times faster than the Nd6 gene fragment. Assuming a 5% cyt *b* rate (as used in this study, and following a similar rate as in Garcia et al., 2011), it results in a 16% ΨCR mutation rate in comparison to such marker, in line with previous estimates of 7.23% (Drovetski, 2003) of the slower evolving CR but closer to the upper bound of 20.2% per MY. This estimate falls within the overall mean of 14.8% (Wenink et al., 1996; Merilä et al., 1997; Hailer et al., 2007) as used for other birds of prey (Hull and Girman, 2004).

3.3. Mitochondrial and nuclear ML networks

Genetic diversity and richness is contrasting between the much faster evolving mitochondrial genes than the nuclear ones. The number of segregating sites being significantly reduced in the nuclear data. All nuclear markers recovered a star-like network structure, with the exception of the more rapidly evolving FIB gene fragment (Fig. 1), suggesting a population expansion. Haplotypes for all nuclear genes are linked among them by not more than one mutation, and networks did not exhibit any clear differentiation for the different buzzard groups. The mitochondrial ML network structuring broadly agrees with *Buteo* spp. systematic arrangement: *hemilasius* (dark blue) is clearly a distinct entity to the remaining buzzards, with high divergence; *rufinus* (light blue) is more closely associated to *buteo* (red) but there is also some divergence between the two taxa; *cirtensis* (green) is recovered within a branch of *buteo* (with 2 haplotypes); all *vulpinus* (orange) are recovered within *buteo* (5 haplotypes) (Fig. 1).[2] The highest genetic diversity within all *Buteo* was found in *vulpinus* from Russia and Ukraine equally, followed by *hemilasius* (Altai and Tuva, respectively) and *buteo* (Slovenia and Portugal, respectively) (Table 1).

3.4. Biogeographical appraisal from mitochondrial data

The MCC Bayesian discrete (Fig. 2) and continuous (Fig. 3, SM Fig. 2) mitochondrial trees recovered three well supported

[2] For colour reference for Fig. 1 see the web version of this article.

Table 1
Species, country, number of individuals, number of haplotypes, haplotype and nuclear diversity (with standard deviation) from the concatenated mitochondrial data set.

Species	Country	n	*h*	Hd (± SD)	π (± SD)
buteo	Slovenia	7	4	0.8571 ± 0.1023	0.00100 ± 0.000809
	Bulgaria	9	4	0.7500 ± 0.1121	0.001343 ± 0.000970
	Portugal	37	9	0.8498 ± 0.0324	0.001901 ± 0.001164
	Germany	24	10	0.7464 ± 0.0907	0.001138 ± 0.000791
vulpinus	Russia	2	2	1.000 ± 0.5000	0.001511 ± 0.001850
	Ukraine	3	3	1.000 ± 0.2722	0.001511 ± 0.001424
rufinus	West Kahakstan	18	4	0.4771 ± 0.1338	0.000400 ± 0.000391
	East Kazhakstan	18	4	0.3987 ± 0.1379	0.000326 ± 0.000344
hemilasius	Tuva	41	8	0.8415 ± 0.0338	0.003467 ± 0.001930
	Dauria	4	2	0.6667 ± 0.2041	0.001008 ± 0.000925
	Altai	6	4	0.8667 ± 0.1291	0.001411 ± 0.001078

monophyletic clades; the *Buteo buteo* complex (*buteo*, *vulpinus*, and including *cirtensis* as it groups within this complex) sister clade and to *rufinus* and *hemilasius* as the ancestral clade. Within the *Buteo buteo* complex, all *cirtensis* from South Morocco, Tunisia and Algeria are monophyletic and grouped with *buteo* from Portugal; *vulpinus* is paraphyletic within the *Buteo buteo* complex. The Bayesian Inference (SM Fig. 3) of haplotypes recovered the same tree topology as the BEAST trees, with *hemilasius* ancestral and a weak node support for the sister clade relationship between *rufinus* and the remaining *Buteo* spp. (BPP: 0.73).

3.5. Demographic analysis using mitochondrial data

Unimodal mismatch distributions are consistent with rapid expansion of populations (SM Fig. 4). Goodness-of-fit tests of observed compared to simulated data were non-significant and showed a very high SDD and non-significance (SM Table 5): *buteo* (n = 77, SSD 0.01, p = 0.76), *rufinus* (n = 41, SSD 0.009, p = 0.15) and *hemilasius* (n = 48, SSD 0.003, p = 0.61); therefore the null hypothesis of population expansion could not be rejected. Negative Fu's F and Tajima D for all groups compared and high significance of Fu's F, with the exception of *hemilasius*, give further support for a demographic expansion scenario. Statistical analysis of Bayesian Skyline plots (BSP) of *buteo* (n = 77), *rufinus* (n = 41) and *hemilasius* (n = 48) suggest expansions

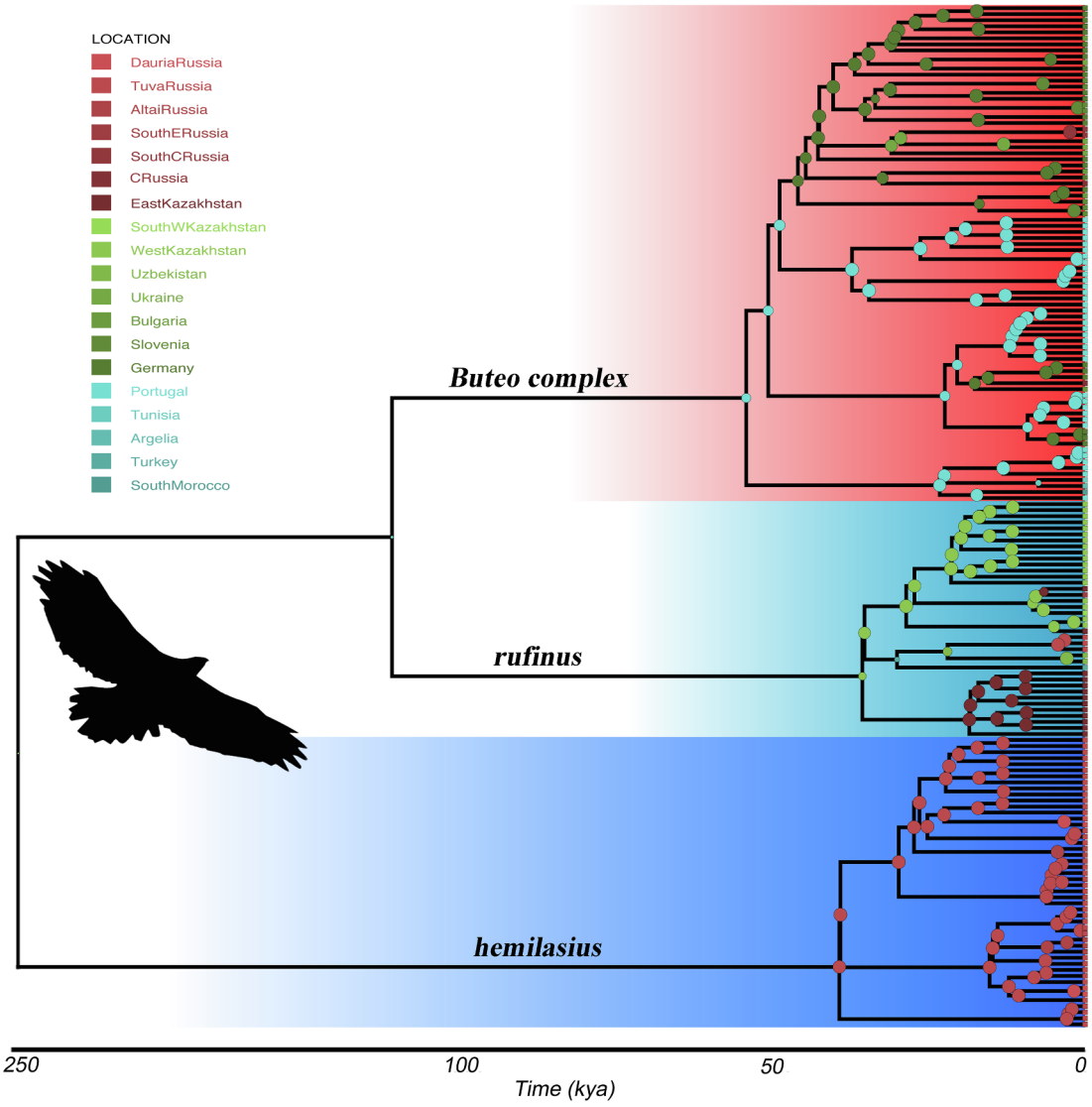

Fig. 2. MCC discrete coalescent tree (n = 169) of *Buteo sp*. Node circles are colour coded by localities and sizes correspond to probability of the locality origin. Red clade; *Buteo buteo* species complex, light blue; *Buteo r. rufinus*, dark blue clade; *Buteo hemilasius.* (For interpretation of the references to colour in this figure legend, the reader is referred to the web version of this article.)

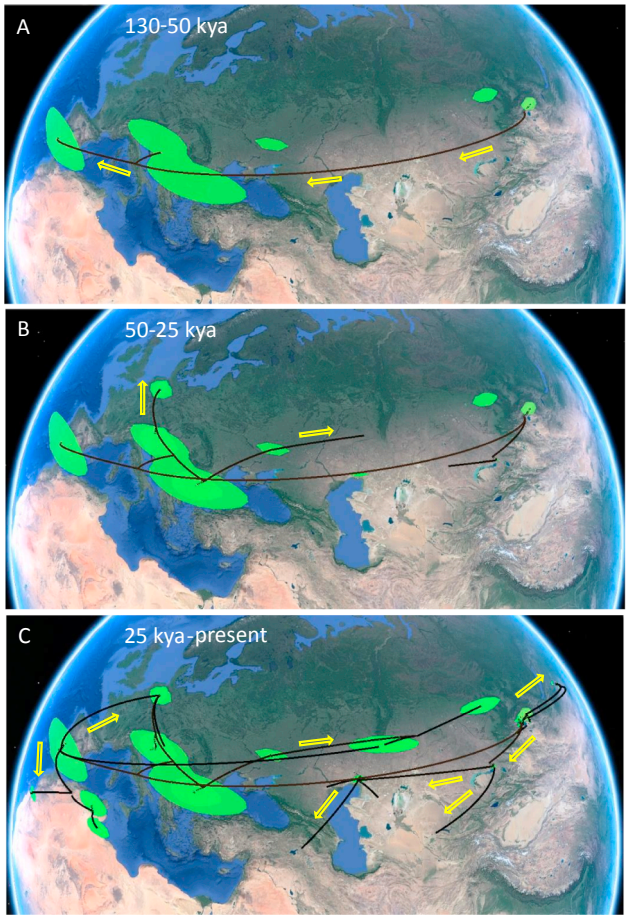

Fig. 3. MCC continuous Bayesian phylogeographic projections of *Buteo* spp. at different times scales: A: 130–50 kya, B: 50–25 kya., C: 25 kya-present. The MCC gene tree is represented with black lines. Polygons represent population areas and are shown in light green. Yellow outlined arrows delimit direction of expansion. (For interpretation of the references to colour in this figure legend, the reader is referred to the web version of this article.)

of all populations but only *rufinus* shows an important population increase. Expansions range from approximately 1500 years for *buteo*, 2000 years for *hemilasius* and 5000 for *rufinus* (SM Fig. 5). These analyses could not be assessed for *vulpinus* and *cirtensis* due to low sample sizes.

AMOVAs of the mitochondrial dataset revealed high variation among populations assigned as 1: *buteo, rufinus, hemilasius*, and 2: *cirtensis, rufinus, buteo* and *hemilasius*, reflecting strong population structure between species or subspecies. Dividing the nominal *buteo* into three geographical regions (Slovenia, Germany and Portugal) revealed high genetic differentiation within rather than between populations, indicating a lack of geographic structure throughout and population admixture (SM Table 6).

3.6. Diversity, differentiation and population structure inferred from fast-evolving markers

Two microsatellites (Bbu51 and BswD223w) showed evidence of null alleles and were discarded. The remaining 20 loci had not evidence of linkage disequilibrium or departure from expectations under Hardy–Weinberg equilibrium and were used for the subsequent analysis. Estimates of allelic richness were similar for the five taxa with a mean value of AR = 4.7. The mean expected heterozygosity (He) was highest in *vulpinus* (0.621) and lowest in *cirtensis* (0.558) although standard error overlaps this difference (Table 2). Overall, results for

Table 2
Species, allelic richness (AR), observed heterozygosity (Ho), expected heterozygosity (He) and inbreeding coefficient (FIS). Standard deviation is given in parenthesis.

	AR	Ho (s.d.)	He (s.d.)	FIS
buteo	4.78	0.552 (0.272)	0.590 (0.279)	0.048
cirtensis	4.62	0.506 (0.294)	0.558 (0.295)	0.092
vulpinus	4.30	0.599 (0.302)	0.621 (0.222)	0.038
rufinus	4.97	0.565 (0.227)	0.614 (0.258)	0.068
hemilasius	4.80	0.581 (0.298)	0.604 (0.295)	0.019

FST and RST differentiation indexes were congruent. The greatest degree of genetic differentiation based on RST was observed between *vulpinus* and all other taxa (*hemilasius* RST = 0.386, $p < 0.001$; *cirtensis* RST = 0.243, $p < 0.001$; *buteo* RST = 0.175, $p < 0.001$; *rufinus* RST = 0.175, $p < 0.001$), suggesting recent low gene flow between the *vulpinus* and all other taxa. The FST did not recover such divergence, with *buteo* and *vulpinus* recovering very low FST value (FST = 0.011, not significant) and *buteo* being not significantly different from *cirtensis*. All other comparisons were highly significant (SM Table 7).

The extent of geographical structuring inferred from the microsatellite data between both assigned groups (group 1: *buteo, cirtensis, vulpinus*, and *rufinus*, and group 2: *hemilasius*) reveals that most of the variation for fast-evolving markers lies within individuals for both distance methods used (variation $_{FST}$ = 89.2%; variation $_{RST}$ = 74.9%), a likely consequence of recent high gene flow within and among the assigned groups (SM Table 8). However, using the RST distance method we also observed an important fraction of differentiation among groups (13.2%).

The results of the Bayesian clustering analysis of multilocus genotypes showed that the mean log likelihood [(ln P (D/K)] for the assumed number of clusters peaked at K = 3 and K = 5, the latter exhibiting a large variance. The ad hoc statistic, ΔK (Evanno et al., 2005), showed a single peak at K = 3 (SM Fig. 1). We therefore considered K = 3 to be the most likely number of independent evolutionary units present in the dataset. These 3 clusters represent (i) *hemilasius*, (ii) *rufinus*, and (iii) *buteo* + *vulpinus*. Individual assignment to the three clusters evidence geographical concordance and indicate the presence of clear contact zones where taxa meet geographically. Individuals classified morphologically as *cirtensis* do not form a separate cluster, and are apparently composed by admixed genomes between *rufinus* and *buteo* + *vulpinus* (Fig. 4).

In agreement with the biogeographic and phylogenetic data, and with Bayesian analysis of population structure, the results from the Discriminant Analyses of Principal Components (DAPC) revealed three clear clusters (1: *hemilasius*, 2: *rufinus* and 3: *Buteo buteo* complex (*buteo, vulpinus, cirtensis*)). Within the *B. buteo* complex, *cirtensis* remains less inclusive in the group with reduced spatial overlap (SM Fig. 6) suggesting some level of distinct genetic differentiation to *buteo* and *vulpinus*, certainly as a result of introgression with *rufinus* with which is juxtaposed for the second principal component.

3.7. Demographic analysis using microsatellite data

Results from the Extended Bayesian Skyline Plots of the microsatellites (EBSP) revealed that the effective population sizes for *hemilasius*, *rufinus*, and *vulpinus* have remained relatively constant for at least the last 10 kya (Fig. 5). In contrast, *cirtensis* has a more recent population history (~6 kya) and has undergone a dramatic population expansion within approximately the last 3 kya (an 11 (Mean Ne) and 7.6 (Median Ne) fold population expansion). In two taxa, *hemilasius* and *rufinus*, we detected strong signatures of very recent bottlenecks, with one of them (*rufinus*) showing signs of recovery. A similar signature of bottleneck with recovery can also be read in the EBSP of *vulpinus*, although the 95% HPD (highest posterior density) estimates suggest that

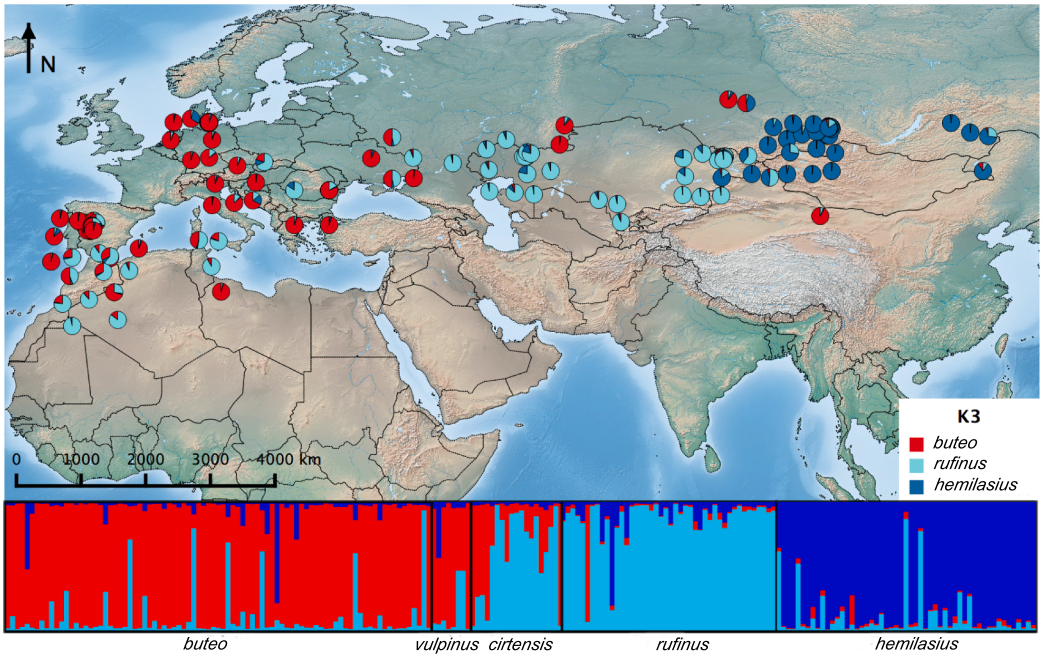

Fig. 4. Map of all Buzzard (*Buteo* spp.) specimens sampled across the distribution ranges. Pie charts are Bayesian estimates of assignment for each individual at K = 3 based on the analysis of 20 microsatellites.

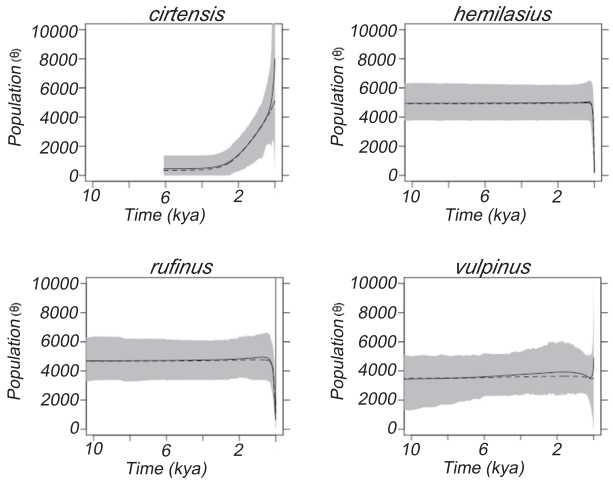

Fig. 5. Microsatellite extended Bayesian Skyline Plot (EBSP) of *Buteo b. cirtensis* (comb. nov.), *B. b. vulpinus, B. r. rufinus* and *B. hemilasius*. Time is given in years.

the pattern is overall constant. Due to the very low Effective Sample Size (ESS) from the *buteo* data set, we could not analyse its demography.

4. Discussion

4.1. Phylogeography

Our findings of the timings of expansions and contractions in *Buteo* spp. and their populations concur with other avian species range shifts in the West Palearctic, ranging from the Middle Pleistocene to the Late Pleistocene/Holocene transition (Holm and Svenning, 2014), which have been primarily linked to changes in vegetation in response to climate change. These avifaunal responses to climate change are reflected in phenology and population dynamics as is apparent in *Buteo* spp. Times of divergence are aimed to establish approximate times of speciation in a broad sense and therefore caution is needed in the interpretation, more so when dating lies within the highly changeable Pleistocene climate conditions.

Speciation or divergence events between the *B. buteo* complex (*buteo, vulpinus, cirtensis)* and *rufinus* (107–119 kya) point to a time of transition between colder and warmer climate conditions (Fig. 3). The Riss-Würm interglacial (130–115 kya, MIS5) or Eemian Interglacial (in Mediterranean Europe, 126–110 kya, Sánchez Goñi et al., 1999) has been estimated for a length of circa 17.5 kya (see Helmens, 2013). This warmer climate allowed forests to replace tundra at higher latitudes and new habitats became available for new populations to expand, contributing to novel colonization events. The contrasting ecological niche requirements of *B. buteo* subspecies (low altitude forest edge) and *rufinus* (steppe or semi-desert) likely contributed to distributional shifts of their populations. Similarly, warmer conditions throughout the Mindel-Riss (380/330–200 kya) are likely to have contributed to divergence between *hemilasius* and the *B. buteo* complex (*buteo, vulpinus, cirtensis)* and *rufinus* circa 250–232 kya by expanding to new habitats. Several studies have shown that cold-adapted species have larger populations during glaciation periods and reduced populations during interglacials (Shapiro et al., 2004; Dalén et al., 2005). It is apparent that climatic conditions affect species habitat shifts differently (Stewart et al., 2010). Climate change in resident cold-adapted montane steppe species such as *hemilasius* may have had a reduced or limited impact on its populations but likely contributed to the expansion of other *Buteo* species.

The MCC 95% HPD mean time estimates for *hemilasius* (27–40 kya), *rufinus* (33–40 kya) and *B. buteo* complex (52–59 kya) clades fall ahead of LGM at around the MIS 3 (57–29 kya, Helmens, 2013; 60–27 kya, Van Meerbeeck et al., 2009) and thus suggests population contractions throughout this period of cool climate and abrupt temperature rises. Paleoclimatic and vegetation evidence suggests that during this time, climatic conditions would have been suited for tundra-steppe vegetation across all Europe and Eurasia (Peyron et al., 1998; Holm and Svenning, 2014) and that these species would have been distributed throughout, as has been suggested for other raptors (Garcia et al., 2011). These contractions date to the cooler temperatures of the High Weichselian Glacial (57–15 kya) with prevailing polar desert and steppe-tundra and trees at southern refugia (Van Andel and Tzedakis, 1996). Nevertheless, the rapid fluctuating climatic changes throughout

this period (Rasmussen et al., 2014) and the large distribution range of *rufinus*, *buteo* and *vulpinus* suggest complex and multiple population shifts throughout the range, possibly more severe at peripheral populations. However, the timing of *B. buteo* complex lies within hotter temperatures compared to those of *hemilasius* and *rufinus* and may suggest contractions at glacial times following forest expansions.

Buteo rufinus fossil remains in England dating to this period (40–50 kya, Stewart and Jacobi, 2015) and in France, Luxembourg and Northern Spain (Mourer-Chauviré, 1975; Elorza, 1990; Tyrberg, 1998; Holm and Svenning, 2014) throughout the cold Late Pleistocene are further evidence of past expansions under colder conditions and today's reduced populations. Furthermore, *Buteo buteo* subfossils in southern and eastern Europe and in the Middle East date to times of interchanging glacial-interglacial conditions or to either of them (Elorza, 1990).

The vegetation cover throughout the LGM (18 kya) in central Asia and southern-eastern Europe was mainly steppe with areas of intergradation composed of tundra-steppe (Tarasov et al., 2000; Elenga et al., 2000). This vegetation changed during the drier Holocene (circa 10 kya) as a consequence of temperate forest expansions in Europe and taigas in Asia (Novenko et al., 2009), and has been suggested to have contracted steppe associated avian populations (Garcia et al., 2008). Throughout the Holocene however, there were repeated periods of climate change (roughly every 0.6–1 kya, Mayewski et al., 2004) with drier steppe vegetation expansions during short glacial conditions (11.5–9.5, 8–7 and 4–3 kya) where steppe-like communities may have thrived (Sorrel et al., 2007). The moister Mid Holocene (6 kya) circum-Mediterranean region underwent progressive aridification. Interestingly, the most important climatic changes are seen in northern Africa by changes in the seasonable climate (see Prentice et al., 2000). Furthermore, the Altai–Sayan mountain region has been suggested to be a recent refugium of mammals during the LGM (Řičánková et al., 2015) with similar ecological structure and fauna to those of the Pleistocene and Holocene (Agadjanian and Serdyuk, 2005; Řičánková et al., 2014). The three most important mammal Holocene retractions in Europe and in the rest of the Palearctic region were in the Altai-Sayan, followed by the Kazakhstan and eastern plains refugia and point to important areas of likely genetic divergence (Řičánková et al., 2014; Řičánková et al., 2015). Clues from *Buteo* refugia may derive from areas of higher genetic diversity at localities, such as for *hemilasius* (Altai and Tuva), *vulpinus* (Russia and Ukraine), and *buteo* (Slovenia and Portugal).

Several studies have found a genetic distinction between western and eastern raptor populations in the Palearctic (Godoy et al., 2004). Nittinger et al., (2007) found two haplotypes, one East and another West, in *Falco cherrug* (previously *F. c. cherrug* to the West and *F. c. milvipes* to the East). They argued that a postglacial expansion route of the western haplotype from West to the northeast followed the lower steppe areas to northern Kazakhstan, to the Altai Mountains and to Mongolia and Northern China. A contact zone with the other haplotype from *Falco rusticolus* formed hybrids in the area; a posterior southern expansion carried this new haplotype South.

The assumption of a range expansion is compatible with the finding of significant deviation from neutral expectations (negative Tajima's D) for *buteo, vulpinus* and *rufinus.* The finding of non-significant deviation observed in other groups but with negative values corroborate similar findings. Results from the extended Bayesian Skyline plots suggest a recent arrival of *cirtensis* to North Africa and coincides with rapid aridification in the Maghreb region, circa 6 kya. However, the low node support and sample size calls for caution with this interpretation. Interestingly, the first records of *cirtensis* arriving from Morocco to breed in the Iberian Peninsula, date to the present century, and are believed to be a response to global warming (Araújo et al., 2011; Chamorro et al., 2017). Growing evidence of species' responses to past climatic changes (Root, 1998; Huntley and Webb, 1989) strongly indicate a similar habitat shift pattern in avian fauna to ongoing and future climate change (Sanz, 2002; Parmesan, 2006; Huntley et al., 2008). Further expansions of buzzards to Europe were likely influenced by anthropogenic landscape transformations in the Neolithic (Diamond and Bellwood, 2003; Price and Bar-Yosef, 2011) and the creation of new steppe habitats for species to colonize or expand their distributional ranges (O'Connor and Shrubb, 1986; Bouma et al., 1998; Ruddiman, 2003). Geographical shifts in *rufinus* nesting grounds have been recorded in Israel in the last four decades as a consequence of anthropogenic disturbance (Friedemann et al., 2011). Thus, paleoclimatic data and the effect of human impact are likely factors that have influenced the occurrence of contact zones in buzzards through population gene flow and admixture.

4.2. Differentiation, introgression and systematics

Our findings corroborate previous studies showing high levels of divergence between *hemilasius* and *rufinus* based on the rapid evolving ΨCR sequence in *Buteo* species (Haring et al., 1999; Kruckenhauser et al., 2004) that were originally considered as conspecifics (Hartert, 1914; Meinertzhagen, 1954). Such phylogeographic work showed the recovery of the same haplotypes between *rufinus* and the African *oreophilus,* and also between *buteo* and *vulpinus*, showing a clear lack of geographical structure and genetic differentiation between them. This finding is surprising as geographical distances between subspecies could range thousands of kilometers. In the light of such findings *buteo*, *rufinus* and *oreophilus* are thought to have arisen from a recent radiation, and *buteo*, *vulpinus*, *rufinus* and *oreophilus* are considered to form one superspecies (Haring et al., 1999). Similarly, our results are in agreement with the previous studies that show low genetic differentiation between *B. buteo* subspecies and *rufinus*, suggesting the role of Pleistocene ice ages to promote gene flow by expansion and contraction through changing environmental conditions (Haring et al., 1999). This assumption falls in chronological concordance with the earliest fossil findings of both species (Isturitz, Spain) ascribed to the Würm II/III period (64–10 kya) (Elorza, 1990).

The mitochondrial analyses support the genetic differentiation between *rufinus* and *cirtensis,* in congruence with morphological data supporting a distinction between them (Kruckenhauser et al., 2004). Nevertheless, Kruckenhauser et al.'s (2004) main morphological character relied on an environmental condition trait (size), which may not be an indication of actual differentiation per se. Their results on the phylogeographic relationships, based on their ΨCR network on *Buteo* subspecies (*buteo* and *vulpinus*), show a clear unresolved positioning of *cirtensis* and *buteo* subspecies. Our data shows a two-time (past and present) relationship on the positioning of *cirtensis*. Historical or ancestral relationships as inferred from the mitochondrial data groups *cirtensis* within the *B. buteo* species complex. Interestingly, all *cirtensis* are monophyletic and are grouped with a few individuals of *buteo* from southern Portugal. In accordance, the microsatellite data shows gene flow between both forms (*buteo* and *cirtensis*).

West Paleartic Buzzards are thought to have evolved within a short time frame, possibly through the reduction of ranges during glacial stages resulting in population admixture. However, Kruckenhauser et al. (2004) suggest a likely glacial bottleneck reducing mitochondrial diversity in *vulpinus, trizonatus* and *cirtensis*, supporting Schreiber et al. (2001) low allozyme heterozygosity despite polymorphism plumage in *buteo* morphs. As discussed by Kruckenhauser et al. (2004), the morphological similarity between *rufinus* and *hemilasius* has been considered by others (Hartert, 1914; Del Hoyo et al., 1994) as indicative of close relationship, but was not supported by their morphological analyses and is not supported in this study or in other genetic work (Haring et al., 1999). Results from our phylogenetic relationships do not concur with the current taxonomical classification suggested by Kruckenhauser et al. (2004) and the nomination of *cirtensis* as *B. r. cirtensis.* However, we suggest that, in accordance to the phylogenetic species concept, *B. r. cirtensis* should be an allospecies of the *B. buteo* superspecies complex (*Buteo buteo cirtensis*).

The nuclear sequences data resulted to be much less informative than the mitochondrial data set to assess divergence. This, at first, can be confusing and may suggest a male-biased dispersal though male raptors philopatric tendency suggests otherwise. However, the much more conserved nuclear markers would point more to shared polymorphisms and indicate a recent common gene pool for all three nominal species. Here, ancestral polymorphism of the population makes unclear the possible effect of gene flow and/or the presence of re-occurring admixture events in the distributional ranges of the different morphs. The discrepancy between the mtDNA and microsatellite data is expected, given the four-fold effective population size of nuclear genes, the much higher mutation rate of microsatellites and the enhanced genetic drift of mtDNA in comparison to nuclear markers (Birky et al., 1983). Such variation needs not to be the outcome of sex-biased dispersal, and can be accounted by the mode of inheritance and mutation rate alone.

Admixture events cannot be ruled out between all forms (*buteo*, *vulpinus*, *cirtensis*, *rufinus* and *hemilasius*). All of them share some degree of overlap in their breeding areas (Haring et al., 1999) and the sighting and reports of mixed forms and likely hybrids are well documented (see Elorriaga and Muñoz, 2013). Admixed individuals have been identified in the Straits of Gibraltar, Turkey, Algeria, Tunisia and Italy (Elorriaga and Muñoz, 2013). The case of *cirtensis* is interesting because the first records of breeding in southern Iberia date only to 2009. However, previous attempts to unravel *cirtensis* taxonomy are unclear and even museum samples from Algeria and Tunisia have shown to be intermixed with other Palearctic *Buteo*, suggesting admixture that went unnoticed for nearly a century (Kruckenhauser et al., 2004). This is confirmed by our more extensive sequence data where all *cirtensis* from Morocco, Tunisia and Algeria, both museum and fresh samples, clustered within the *buteo* haplogroup. The microsatellite data do not show either an independent entity representing *cirtensis*, but rather individuals are an admixture of *buteo* and *rufinus* with slightly closer relationships with the latter. However, one attributed *cirtensis* from Portugal (BT2) clustered within the network with the three assigned *cirtensis* (Tunisia, Morocco and Argelia) suggesting distinct morphological traits in *cirtensis*. This is the first molecular confirmation of this taxon's presence in the Iberian Peninsula. The high number of haplotypes recovered from *vulpinus* from the sequence data suggest some distinction of this form. Sequence and genotype data revealed introgression of *hemilasius* and *buteo* in *rufinus*, suggesting gene flow within the populations at their contact zones. It is unclear if the presence of contact zones will have important consequences in the buzzard populations preventing speciation or enhancing it through reinforcement.

Admixture between taxa at contact zones (e.g., *hemilasius – rufinus*, or *buteo – rufinus, buteo – vulpinus*) may be maintained by sexual imprinting of nestlings on the plumage pattern of the parent morph that spends the longest time in the nest (Cramp and Simmons, 1980). In the Common buzzard (*buteo*), morphological plumage polymorphism (light, dark, intermediate) is maintained through heterozygote advantage through assortative mating, thus non-random mate selection. This behaviour is believed to be maladaptive for presumed homozygous morphs where nestlings assume their future mate by imprinting on the mother's morph (Krüger et al., 2001). We are unaware if this mate selection model system has been reported in other birds since the above publication, but at the time it was believed to be novel and unique and may therefore be intrinsic to the extreme morphological variability and taxonomical difficulty in buzzards. Furthermore, lack of genetic structure to differentiate between species at the nuclear level may suggest that phenotypic and morphological traits have evolved in a short time scale in response to fast adaptations to changing environmental conditions and hunting behavior (Bulgin et al., 2003; Zink, 2004). Pererva and Grazhdankin (1994) showed that some birds of prey have undergone rapid phenotypical change this century (*Falco cherrug, Accipiter gentilis, Aquila nipalensis, Aquila heliaca*). Furthermore, Common buzzard populations are thought to be shifting habitat following vole populations (Krüger, 2000, 2004) and this points to the behavioural plasticity in buzzards.

5. Conclusion

The findings of this study reveal a complex pattern of cladogenetic events and population contractions in Palearctic *Buteo* species throughout the Pleistocene, which likely reflect habitat change and contrasting ecological niche requirements between open-habitat species, such as *rufinus* and *hemilasius*, and the forms of more forested habitats from the *B. buteo* complex (*buteo*, *vulpinus*). Phylogenetic analyses inferred from the mitochondrial data recover *hemilasius* as sister taxa to the sister clades of *rufinus* and the *B. buteo* complex (*buteo*, *vulpinus*, *cirtensis*). The positioning of *cirtensis* in the MCC trees denotes its incorrect taxonomic status, and thus we propose an amendment to *Buteo buteo cirtensis*. However, extensive sampling throughout *cirtensis* range (e.g. Tunisia, Egypt and Middle East) should help clarify further its taxonomical status. The slower evolving nuclear loci reveal unresolved genetic entities suggesting a recent common gene pool for all buzzards in congruence with ongoing speciation processes between species. Results from the EBSP reveal that the effective population sizes for *hemilasius*, *rufinus* and *vulpinus* have remained relatively constant throughout the Holocene. In contrast, *cirtensis* has undergone a dramatic population expansion within approximately the last 3 kya. Evidence of population admixture is observed from microsatellite data between all taxa, mostly between *cirtensis* and *buteo* and between *rufinus* and *hemilasius* in congruence with increasing reports of hybridization between species at contact zones and due to habitat shifts. Overall, the findings reflect on the complexity of historical and ongoing intrinsic evolutionary processes contributing to speciation patterns in Palearctic buzzards.

6. Data accesibility

Custom R scripts are available from SS-R, https://github.com/santiagosnchez. Sequences have been deposited under Genbank accession numbers (PENDING). Multiplex genotypes are available from the authors.

Acknowledgements

We are grateful to the following people for providing samples: R El Khamlichi, D Charlotte, A Corso, R Caratão, P Melo and CRASSA, L Barosa, D Costa and GREFA; N Chakarov and the Department of Animal Behaviour, Bielefeld University, Slovenia; A Verses and the National Institute of Biology, Ukraine, S Viter, S Domashevski, D Pale, O Ostrovski, N Tcherkas, M Pestov, A Moshkin and E Shnaider. Thanks to A Muñoz-Merida for providing scripts for file managing. Special thanks to S Mourão and P Ribeiro for their lab assistance. Funding: This work was partially supported by the EDP Biodiversity Chair to PB and by project NORTE-01-0145-FEDER-000007, supported by Norte Portugal Regional Operational Programme (NORTE2020), under the PORTUGAL 2020 Partnership Agreement, through the European Regional Development Fund (ERDF). MJJ owned a research contract (SAESCTN-PIIDT/1/2011, UID/BIA/50027/2013) from ON.2–North Portugal, National Strategic Reference Framework, European Regional Development Funding, and was also supported by a fellowship from the Portuguese Foundation for Science and Technology (FCT, SFRH/BPD/109148/2015) and RG was supported by a research contract from FCT (IF/00564/2012) and from ICETA/UP.

Author contributions

The study was designed by LP, PB, RG. SL generated the data. MJJ, SS-R, RG conducted all analyses, IK, VD, AQ, TV, NO, LP conducted the collecting and/or gathering of samples. MJJ wrote the manuscript with

inputs from of SS-R, PB, LP, RG and NF.

Appendix A. Supplementary material

Supplementary data to this article can be found online at https://doi.org/10.1016/j.ympev.2019.02.004.

References

Agadjanian, A.K., Serdyuk, N.V., 2005. The history of mammalian communities and paleogeography of the Altai Mountains in the Paleolithic. Paleont. J. 39, 645–821.

Aldhebiani, A.Y., 2017. Species concept and speciation. Saudi J. Biol. Sci. 25, 437–440.

Araújo, M. B., del Dedo-Garcimartín, M., Pozo, I., Calmaestra, R. G., 2011. Impactos, vulnerabilidad y adaptación al cambio climático de la biodiversidad española. 2. Fauna de Vertebrados. Madrid: Dirección General de Medio Natural y Política Forestal, Ministerio de Medio Ambiente y Medio Rural y Marino y Museo Nacional de Ciencias Naturales.

Arbogast, B.S., Drovetski, S.V., Curry, R.L., Boag, P.T., Seutin, G., Grant, P.R., Grant, B.R., Anderson, D.J., 2016. The origin and diversification of Galapagos Mockingbirds. Evolution 60, 370–382.

Avise, J.C., 1997. Space and time as axes in intraspecific phylogeography. 381–388. In: Huntley, B., Cramer, W., Morgan, A.V., Prentice, H.C., Allen, J.R.M. (Eds.), Past and Future Rapid Environmental Changes: The Spatial and Evolutionary Responses of Terrestrial Biota. Springer-Verlag, Berlin.

Avise, J.C., Walker, D., Johns, G.C., 1998. Speciation durations and Pleistocene effects on vertebrate phylogeography. Proc. R. Soc. Lond. B 265, 1707–1712.

Baele, G., Lemey, P., Bedford, T., Rambaut, A., Suchard, M.A., Alekseyenko, A.V., 2012. Improving the accuracy of demographic and molecular clock model comparison while accommodating phylogenetic uncertainty. Mol. Biol. Evol. 29, 2157–2167.

Barraclough, T.G., Nee, S., 2001. Phylogenetics and speciation. Trends Ecol. Evol. 16, 391–399.

Bielejec, F., Rambault, A., Suchar, M.A., Lemey, P., 2011. SPREAD: spatial phylogenetic reconstruction of evolutionary dynamics. Bioinformatics 27, 2910–2912.

BirdLife International, 2019. IUCN Red List for birds. Downloaded from http://www.birdlife.org on 02/01/2019.

Birky, C.W., Maruyama, T., Fuerst, P., 1983. An approach to population genetic and evolutionary genetic theory for genes in mitochondria and chloroplasts, and some results. Genetics 103, 513–527.

Blacket, M.J., Robin, C., Good, R.T., Lee, S.F., Miller, A.D., 2012. Universal primers for fluorescent labelling of PCR fragments – an efficient and cost-effective approach to genotyping by fluorescence. Mol. Ecol. Res. 12, 456–463.

Boerner, M., Krüger, O., 2008. Aggression and fitness differences between plumage morphs in the common buzzard (*Buteo buteo*). Behav. Ecol. 20, 180–185.

Bonin, A., Bellemain, E., Bronken Eidesen, P., Pompanon, F., Brochmann, C., Taberlet, P., 2004. How to track and assess genotyping errors in population genetics studies. Mol. Ecol. 13, 3261–3273.

Bouma, J., Varallyay, G., Batjes, N.H., 1998. Principal land use changes anticipated in Europe. Agric. Ecosys. Environ. 67, 103–119.

Bulgin, N.L., Gibbs, H.L., Vickery, P., Baker, A.J., 2003. Ancestral polymorphisms in genetic markers obscure detection of evolutionarily distinct populations in the endangered Florida grasshopper sparrow (*Ammodramus savannarum floridanus*). Mol. Ecol. 12, 831–844.

Chakarov, N., Boerner, M., Krüger, O., 2008. Fitness in common buzzards at the cross-point of opposite melanin–parasite interactions. Funct. Ecol. 22, 1062–1069.

Chamorro, D., Olivero, J., Real, R., Muñoz, A.-R., 2017. Environmental factors determining the establishment of the African Long-legged Buzzard *Buteo rufinus cirtensis* in Western Europe. Ibis 159, 331–342.

Clark, P.U., Dyke, A.S., Shakun, J.D., Carlson, A.E., Clark, J., Wohlfarth, B., McCabe, A.M., 2009. The last glacial maximum. Science 325, 710–714.

Corso, A., 2009. Successful mixed breeding of Atlas Long-legged Buzzard and Common Buzzard on Pantelleria, Italy, in 2008. Dutch Birding 31, 224–226.

Coyne, J.A., Orr, H.A., 2004. Speciation. Sinauer Associates, Sunderland, MA.

Cramp, S., Simmons, K.E.L., 1980. Handbook of the birds of Europe, the Middle East and North Africa. Oxford Univ. Press, Oxford, UK.

Dalén, L., Fuglei, E., Hersteinsson, P., Kapel, C.M.O., Roth, J.D., Samelius, G., Tannerfeldt, M., Angerbjörn, A., 2005. Population history and genetic structure of a circumpolar species: the Artic fox. Biol. J. Linn. Soc. 84, 79–89.

Del Hoyo, J., Elliott, J.A., Sargatal, J., 1994. Handbook of the Birds of the World, 2. Lynx Edicions, Barcelona.

De Queiroz, K., 2007. Species concepts and species delimitations. Syst. Biol. 56, 879–886.

Diamond, J., Bellwood, P., 2003. Farmers and their languages: the first expansions. Science 300, 597.

Do Amaral, F.R., Sheldon, F.H., Gamauf, A., Haring, E., Riesing, M., Silveira, F.F., Wajntal, A., 2009. Patterns and processes of diversification in a widespread and ecologically diverse avian group, the buteonine hawks (Aves, Accipitridae). Mol. Phyl. Evol. 53, 703–715.

Drovetski, S.V., 2003. Plio-Pleistocene climatic oscilations, Holartic biogeography and speciation in an avian subfamily. J. Biogeogr. 30, 1173–1181.

Drummond, A.J., Rambaut, A., Shapiro, B., Pybus, O.G., 2005. Bayesian coalescent inference of past population dynamics from molecular sequences. Mol. Biol. Evol. 22, 1185–1192.

Drummond, A.J., Suchard, M.A., Xie, D., Rambaut, A., 2012. Bayesian phylogenetics with BEAUti and the BEAST 1.7. Mol. Biol. Evol. 29, 1969–1973.

Dudás, M., Tar, J., Tóhl, I., 1999. Natural hybridisation of Long-Legged Buzzard (*Buteo r. rufinus*) and Common Buzzard (*B. buteo*) in the Hortobagy National Park. Temészet 5–6, 8–10.

Earl, D.A., 2011. Structure Harvester v0.6.7, Available at http://users.soe.ucsc.edu/~dearl/software/structureHarvester.

Elenga, H., Peyron, O., Bonnefille, R., Jolly, D., Cheddadi, R., Guiot, J., Jonson, H., 2000. Pollen-based biome reconstruction for southern Europe and Africa 18,000 yr BP. J. Biogeogr. 27, 621–634.

Elorriaga, J., Muñoz, A.-R., 2013. Hybridisation between the Common Buzzard *Buteo buteo buteo* and the North African race of Long-legged Buzzard *Buteo rufinus* cirtensis in the Strait of Gibraltar: Prelude or preclude to colonisation? Ostrich 84, 41–45.

Elorza, M., 1990. Restos de aves en los yacimientos prehistóricos vascos. Estudios realizados. Munibe 42, 263–267.

Endler, J.A., 1977. Geographic Variation, Geographic Variation, Speciation and Clines. Princeton University Press, Princeton, New Jersey, pp. 26.

Evanno, G., Regnaut, S., Goudet, J., 2005. Detecting the number of clusters of individuals using the software STRUCTURE: a simulation study. Mol. Ecol. 14, 2611–2620.

Excoffier, L., Laval, L., Schneider, S., 2005. Arlequin (version 3.0): an integrated software package for population genetics data analysis. Evol. Bioinfor. Online 1, 47–50.

Excoffier, L., Lischer, H.E.L., 2010. Arlequin suite ver 3.5: a new series of programs to perform population genetics analyses under Linux and Windows. Mol. Ecol. Res. 10, 564–567.

Falush, D., Stephens, M., Pritchard, J.K., 2003. Inference of population structure using multilocus genotype data: linked loci and correlated allele frequencies. Genetics 164, 1567–1587.

Fefelov, I.V., 2001. Comparative breeding ecology and hybridization of eastern and western marsh harriers *Circus spilonotus* and *C. aeruginosus* in the Baikal region of eastern Siberia. Ibis 143, 587–592.

Ferguson-Lees, J., Christie, D.A., 2001. Raptors of the World. Helm Edt, London.

Ferreira, M.A.R., Suchard, M.A., 2008. Bayesian analysis of elapsed times in continuous-time Markov chains. Can. J. Stat. 36, 355–368.

Friedemann, G., Yom-Tov, Y., Motro, U., Leshem, Y., 2011. Shift in nesting ground of the long-legged buzzard (*Buteo rufinus*) in Judea, Israel – an effect of habitat change. Biol. Cons. 144, 402–406.

Fu, Y.-X., 1997. Statistical tests of neutrality of mutations against population growth, hitchhiking and background selection. Genetics 147, 915–925.

Garcia, J.T., Suarez, F., Garza, V., Calero-Riestra, M., Hernandez, J., Pérez-Tris, J., 2008. Genetic and phenotypic variation among geographically isolated populations of the globally threatened Duponťs lark *Chersophilus duponti*. Mol. Phyl. Evol. 46, 237–321.

Garcia, J.T., Alda, F., Terraube, J., Mougeot, F., Sternalski, A., Bretagnolle, V., Arroyo, B., 2011. Demographic history, genetic structure and gene flow in a steppe-associate raptor species. BMC Evol. Biol. 11, 333.

Godoy, J.A., Negro, J.J., Hiraldo, F., Donázar, J.A., 2004. Phylogeography, genetic structure and diversity in the endangered bearded vulture (*Gypaetus barbatus*, L.) as revealed by mitochondrial DNA. Mol. Ecol. 13, 371–390.

Goudet, J., 1995. FSTAT (Version 1.2): A Computer Program to Calculate F-Statistics. J. Hered. 86, 485–486.

Gouy, M., Guindon, S., Gascuel, O., 2010. SeaView version 4: a multiplatform graphical user interface for sequence alignment and phylogenetic tree building. Mol. Biol. Evol. 27, 221–224.

Guo, S.W., Thompson, E.A., 1992. Performing the exact test of Hardy–Weinberg proportions for multiple alleles. Biometrics 48, 361–372.

Haffer, J., 1997. Species concepts and species limits in ornithology. In: In: del Hoyo, J., Elliott, J.A., Sargatal, J. (Eds.), Handbook of the Birds of the World, vol. 2. Lynx Ediciones, Barcelona, pp. 11–24.

Hailer, F., Helander, B., Folkestad, A.O., Ganusevich, S.A., Garstad, S., Hauff, P., Vilà, C., 2007. Phylogeography of the white-tailed Eagle, a generalist with large dispersal capacity. J. Avian Biol. 44, 263–271.

Hansson, B., Hasselquist, D., Tarka, M., Zehtindjiev, P., Bensch, S., 2008. Postglacial colonisation patterns and the role of isolation and expansion in driving diversification in a passerine bird. PLoS ONE 3, e2794.

Haring, E., Riesing, M.J., Pinsker, W., Gamauf, A., 1999. Evolution of a pseudo-control region in the mitochondrial genome of Palearctic buzzards (genus *Buteo*). J. Zool. Syst. Evol. Res. 37, 185–194.

Harpending, H.C., Sherry, S.T., Rogers, A.R., Stoneking, M., 1993. Genetic structure of ancient human populations. Curr. Anthropol. 34, 483–496.

Hartert, E., 1914. Die Vögel der paläarktischen Fauna. Friedlander and Son, Berlin, Germany.

Helbig, A.J., Seibold, I., Kocum, A., Liebers, D., Irwin, J., Bergmanis, U., Bensch, S., 2005. Genetic differentiation and hybridization between greater and lesser spotted eagles (Accipitriformes: *Aquila clanga*, *A. pomarina*). J. Ornithol. 146, 226–234.

Helbig, A.J., 2000. Was ist eine Vogel-'Art'? — Ein Beitrag zur aktuellen Diskussion um Artkonzepte in der Ornithologie. Limicola 14 57–79, 172–184, 220–247.

Heled, J., Bouckaert, R.R., 2013. Looking for trees in the forest: summary tree from posterior samples. BMC Evol. Biol. 13, 221.

Helmens, K.F., 2013. The Last Interglacial-Glacial cycle (MIS 5-2) re-examined based on long proxy records from central and northern Europe. Technical Report TR-13-02. Svensk kärnbränslehantering AB, Swedish Nuclear Fuel and Waste Management Company. 1–59.

Hewitt, G., 1996. Some genetic consequences of the ice ages, and their role in divergence and speciation. Biol. J. Linn. Soc. 58, 247–276.

Hewitt, G., 2000. The genetic legacy of the Quaternary ice ages. Nature 405, 907–913.

Hillel, J., Groenen, M.A.M., Tixier-Boichard, M., Korol, A.B., David, L., Kirzhner, V.M., Weigend, S., 2003. Biodiversity of 52 chicken populations assessed by microsatellite typing of DNA pools. Gen. Sel. Evol. 35, 533–557.

Holm, S.R., Svenning, J.-C., 2014. 180,000 years of climate change in Europe: avifaunal

response and vegetation implications. PlosOne. https://doi.org/10.1371/journal.pone.0094021.t001.
Hull, J.M., Girman, D.J., 2004. Effects of Holocene climate change on the historical demography of migrating sharp-shinned hawks (*Accipiter striatus velox*) in North America. Mol. Ecol. 14, 159–170.
Hull, J.M., Tufts, D., Topinka, J.R., May, B., Ernest, H.B., 2007. Development of 19 microsatellite loci for Swainson's hawks (*Buteo swainsoni*) and other buteos. Mol. Ecol. Notes 7, 346–349.
Huntley, B., Webb, T.I.I.I., 1989. Migration: species' response to climatic variations caused by changes in the earth's orbit. J. Biogeogr. 16, 5–19.
Huntley, B., Collingham, Y.C., Willis, S.G., Green, R.E., 2008. Potential impacts of climatic change on european breeding birds. PlosOne. https://doi.org/10.1371/journal.pone.0001439.
Johnson, P.C.D., Fowlie, M.K., Amos, W., 2005. Isolation of microsatellite loci from the common buzzard, *Buteo buteo* (Aves: Accipitridae). Mol. Ecol. Notes 5, 208–211.
Jombart, T., Devillard, S., Balloux, F., 2010. Discriminant analysis of principal components: a new method for the analysis of genetically structured populations. BMC Genet. 11, 94.
Kass, R.E., Raftery, A.E., 1995. Bayes Factors. J. Am. Stat. Assoc. 90 (430), 773–795.
Knowles, L.L., 2001. Did the Pleistocene glaciations promote divergence? Tests of explicit refugial models in montane grasshoppers. Mol. Ecol. 10, 691–701.
Kruckenhauser, K., Haring, E., Pinsker, W., Riesing, M.J., Winkler, H., Wink, M., Gamauf, A., 2004. Genetic vs. morphological differentiation of Old World buzzards (genus *Buteo*, Accipitridae). Zool. Scripta 33, 197–211.
Krüger, O., 2000. Life history strategies and population dynamics of Common Buzzard Buteo buteo and Goshawk *Accipiter gentilis*. PhD thesis. University of Bielefeld, Germany.
Krüger, O., 2002. Dissecting common buzzard lifespan and lifetime reproductive success: the relative importance of food, competition, weather, habitat and individual attributes. Oecologia 133, 474–482.
Krüger, O., 2004. The importance of competition, food habitat, weather and phenotype for the reproduction of Buzzard *Buteo buteo*. Bird Study 51, 125–132.
Krüger, O., Lindström, J., Amos, W., 2001. Maladaptive mate choice maintained by heterozygote advantage. Evolution 55, 1207–1214.
Lanfear, R., Calcott, B., Ho, S.Y.W., Guindon, S., 2012. PartitionFinder: combined selection of partitioning schemes and substitution models for phylogenetic analyses. Mol. Biol. Evol. 29, 1695–1701.
Lemey, P., Rambaut, A., Drummond, A.J., Suchard, M.A., 2009. Bayesian phylogeography finds its roots. PLoS Comp. Biol. https://doi.org/10.1371/journal.pcbi.1000520.
Lemey, P., Rambaut, A., Welch, J.J., Suchard, M.A., 2010. Phylogeography takes a relaxed random walk in continuous space and time. Mol. Biol. Evol. 27, 1877–1885.
Lerner, H.R.L., Klaver, M.C., Mindell, D.P., 2008. Molecular phylogenetics of the Buteonine birds of prey (Aves, Accipitridae). The Auk 125, 304–315.
Librado, P., Rozas, J., 2009. DNAsp v5: a software for comprehensive analysis of DNA polymorphism data. Bioinformatics 25, 1451–1452.
Löhmus, A., Väli, Ü., 2001. Interbreeding of the Greater *Aquila clanga* and Lesser spotted eagles *A. pomarina*. Acta Ornithol. 4, 377–384.
Nabholz, B., Glémin, S., Galtier, N., 2009. The erratic mitochondrial clock: variations of mutation rate, not population size, affect mtDNA diversity across birds and mammals. BMC Evol. Biol. 9, 54.
Mayewski, P.A., Rohling, E.E., Stager, J.C., Karlén, W., Maasch, K.A., Meeker, L.D., et al., 2004. Holocene climate variability. . Quatern. Res. 62, 243–255.
Mayr, E., 1963. Animal Species and Evolution. Harvard University Press, Cambridge, MA.
McCarthy, E.M., 2006. Handbook of Avian Hybrids of the World. Oxford University Press.
Meinertzhagen, R.I., 1954. Birds of Arabia. Oliver and Boyd, Edinburgh, UK.
Merilä, J., Sheldon, B.C., Ellegren, H., 1997. Antagonistic natural selection revealed by molecular sex identification of nestling collared flycatchers. Mol. Ecol. 6, 1167–1175.
Miller, M.A., Pfeiffer, W., Schwartz, T., 2010. Creating the CIPRES Science Gateway for inference of large phylogenetic trees. In: Gateway Computing Environments Workshop (GCE), 1–8.
Mindell, D.P., Sorenson, M.D., Dimcheff, D.E., 1998. Multiple independent origins of mitochondrial gene order in birds. Proc. Natl. Acad. Sci. USA 95, 10693–10697.
Monti, F., Duriez, O., Arnal, V., Dominici, J.-M., Sforzi, A., Fusani, L.A., Grémillet, D., Montgelard, C., 2015. Being cosmopolitan: evolutionary history and phylogeography of a specialized raptor, the Osprey *Pandion haliaetus*. BMC Evol. Biol. 15, 255.
Morales-Barbero, J., Martinez, P.A., Ferrer-Castán, D., Olalla-Tárraga, M.Á., 2017. Quaternary refugia are associated with higher speciation rates in mammalian faunas of the Western Palaearctic. Ecography. https://doi.org/10.1111/ecog.02647.
Mourer-Chauviré, C., 1975. Les oiseaux du Pléistocène moyen et supérieur de France. Documents de Laboratoires de Géologie de Lyon, 64/2, 624pp.
Nadachowska-Brzyska, K., Burri, R., Smeds, L., Ellegren, H., 2016. PSMC analysis of effective population sizes in molecular ecology and its application to black-and-white *Ficedula* flycatchers. Mol. Ecol. 25, 1058–1072.
Nittinger, F., Gamauf, A., Pinsker, W., Wink, M., Haring, E., 2007. Phylogeography and population structure of the Saker falcon (*Flaco cherrug*) and the influence of hybridization: mitochondrial and microsatellite data. Mol. Ecol. 16, 1497–1517.
Nosil, P., Harmon, L.J., Seehausen, O., 2009. Ecological explanations for (incomplete) speciation. Trends Ecol. Evol. 24, 145–156. https://doi.org/10.1016/j.tree.2008.10.011. pmid:19185951.
Novenko, E.Yu., Glasko, M.P., Burova, O.V., 2009. Landscape-and-climate dynamics and land use in the Late Holocene forest-steppe ecotone of the East European Plain (upper Don River Basin case study). Quatern. Int. 203, 113–119.
O'Connor, R.J., Shrubb, M., 1986. Farming and Birds. Published by Cambridge University Press, Cambridge.
Ortego, J., Aparicio, J.M., Cordero, P.J., Calabuig, G., 2008. Characteristics of loci and individuals are associated with germline microsatellite mutation rates in lesser kestrels (*Falco naumanni*). Mutat. Res. Fund. Mol. Mech. Mut. 648, 82–86.
Parmesan, C., 2006. Ecological and evolutionary responses to recent climate change. Annu. Rev. Ecol. Evol. Syst. 37, 637–669.
Peck, D.R., Congdon, B.C., 2004. Reconcilling historical processes, population structure in the sooty tern *Sterna fuscata*. J. Avian Biol. 35, 327–335.
Pererva, V.I., Grazhdankin, A.V., 1994. Possible effects of anthropogenic environmental changes on morphological variation of some European birds of prey. In: Meyburg, B.-U., Chancellor, R.D. (Eds.), Raptor Conservation Today. WWGBP/Pica Press, Mountfield, Sussex, UK, pp. 667–675.
Peyron, O., Guiot, J., Cheddadi, R., Tarasov, P., Reille, R., de Beaulieu, J.-L., Andrieu, V., 1998. Climatic reconstruction in Europe from 18,000 yr BP from pollen data. Quatern. Res. 49, 183–196.
Prentice, I.C., Jolly, D., 2000. BIOME 6000 participants Mid-Holocene and glacial-maximum vegetation geography of the northern continents and Africa. J. Biogeogr. 27, 507–519.
Pritchard, J.K., Stephens, M., Donnelly, P., 2000. Inference of population structure using multilocus genotype data. Genetics 155, 945–959.
Price, D.T., Bar-Yosef, O., 2011. The origins of agriculture: new data, new ideas. An introduction to Supplement 4. Curr. Anthropol. 52, 163–S174.
Pfänder, P., Schmigalew, S., 2001. Extensive hybridization of Long-legged Buzzard *Buteo r. rufinus* and Upland Buzzard *B. hemilasius*. Ornithologische Mitteilungen 53, 344–349.
Posada, D., 2008. jModelTest: phylogenetic model averaging. Mol. Biol. Evol. 25, 1253–1256.
Pulgarín-R, P.C., Burg, T.M., 2012. Genetic signals of demographic expansion in Downy Woodpecker (*Picoides pubescens*) after the last North American glacial maximum. PlosOne 2012 (7), e40412. https://doi.org/10.1371/journal.pone.0040412.
Rambaut, A., 2014. FigTree v1.4.2: Tree figure drawing tool. http://tree.bio.ed.ac.uk.
Rambaut, A., Drummond, A.J., 2015. TreeAnnotator v1.8.2: MCMC Output analysis. http://beast.bio.ed.ac.uk.
Rambaut, A., Suchard, M.A., Xie, W., Drummond, A.J., 2013. Tracer v.1.6.0: MCMC Trace Analysis Tool. http://beast.bio.ed.ac.uk.
Ramos-Onsins, S.E., Rozas, J., 2002. Statistical properties of new neutrality tests against population growth. Mol. Biol. Evol. 19, 2092–2100.
Randler, C., 2004. Frequency of bird hybrids: does detectability make all the difference? J. Ornithol. 145, 123–128.
Rasmussen, S.O., Bigler, M., Blockley, S.P., Blunier, T., Buchardt, S.L., Clausen, H.B., Cvijanovic, I., Winstrup, M., 2014. A stratigraphic framework for abrupt climatic changes during the Last Glacial period based on three synchronized Greenland ice-core records: refining and extending the INTIMATE event stratigraphy. Quatern. Sci. Rev. 106, 14–28.
Ray, N., Currat, M., Excoffier, L., 2003. Intra-deme molecular diversity in spatially expanding populations. Mol. Biol. Evol. 20, 76–86.
Řičánková, V.P., Robovsky, J., Riegert, J.B., 2014. Ecological structure of recent and Last Glacial Mammalian faunas in Northern Eurasia: the case of Altai, Sayan Refugium. PlosOne e85056.
Řičánková, V.P., Jan, R., Riegert, J., Zrzavý, J., 2015. Regional patterns of postglacial changes in the Palearctic mammalian diversity indicate retreat to Siberian steppes rather than extinction. Sci. Rep. 5, 12682.
Riesing, M.J., Kruckenhauser, L., Gamauf, A., Haring, E., 2003. Molecular phylogeny of the genus *Buteo* based on mitochondrial marker sequences. Mol. Phylogenet. Evol. 27, 328–342.
Rice, W.R., 1989. Analyzing tables of statistical tests. Evolution 43, 223–225.
Rogers, A.R., Harpending, H., 1992. Population growth makes waves in the distribution of pairwise genetic differences. Mol. Biol. Evol. 9, 552–569.
Ronquist, F., Huelsenbeck, J.P., 2003. MrBayes 3: Bayesian phylogenetic inference under mixed models. Bioinformatics 19, 1572–1574.
Root, T., 1998. Energy constraints on avian distributions and abundances. Ecology 69, 330–339.
Ruddiman, W.F., 2003. The anthropogenic greenhouse era began thousands of years ago. Climatic Change 61, 261–293.
Rundle, H.D., Nosil, P., 2004. Ecological speciation. Ecol. Lett. 8, 336–352.
Salzburger, W., Ewing, G.B., Von Haeseler, A., 2011. The performance of phylogenetic algorithms in estimating haplotype genealogies with migration. Mol. Ecol. 20, 1952–1963.
Sambrook, J., Fritsch, E.F., Maniatis, T., 1989. Molecular Cloning: A Laboratory Manual, second ed. Cold Spring Harbor Laboratory Press, New York.
Sánchez Goñi, M.F., Eynaud, F., Turon, J.L., Shackleton, N.J., 1999. High resolution palynological record off the Iberian Margin: direct land-sea correlation for the last interglacial complex. Earth Planet. Sc. Lett. 171, 123–137.
Sanz, J.J., 2002. Climate change and birds: have their ecological consequences already been detected in the Mediterranean region? Ardeola 49, 109–120.
Schreiber, A., Stubbe, A., Stubbe, M., 2001. Common buzzard (*Buteo buteo*): a raptor with hyperpolymorphic plumage morphs, but low allozyme, heterozygosity. J. Ornithologie 142, 34–48.
Shapiro, B., Drummond, A.J., Rambaut, A., Wilson, M.C., Matheus, P.E., Sher, A.V., Cooper, A., 2004. Rise and fall of the Beringian steppe bison. Science 306, 1561–1565.
Silvestro, D., Michalak, I., 2012. RaxmlGUI: a graphical front-end for RAxML. Org. Divers. Evol. 12, 335–337.
Sites Jr, J.W., Marshall, J.C., 2003. Delimiting species: a Renaissance issue in systematic biology. Trends Ecol. Evol. 18, 462–470.
Slatkin, M., Hudson, R.R., 1991. Pairwise comparisons of mitochondrial DNA sequences in stable and exponentially growing populations. Genetics 129 (2), 555–562.
Sorrel, P., Popescu, S.-M., Klotz, S., Suc, J.-P., Oberhänsli, H., 2007. Climate variability in the Aral Sea Basin (Central Asia) during the late Holocene based on vegetation

changes. Quatern. Res. 67, 357–370.
Stewart, J.R., Lister, A.M., Barnes, I., Dalén, L., 2010. Refugia revisited: individualistic responses of species in space and time. Proc. R. Soc. Lon. 277, 661–671.
Stewart, J.R., Jacobi, R.M., 2015. The long term response of birds to climate change: new results from a cold stage avifauna in Northern England. PlosOne. https://doi.org/10.1371/journal.pone.0122617.
Taberlet, P., Fumagalli, L., Wust-Saucy, A.-G., Cosson, J.-F., 1998. Comparative phylogeography and postglacial colonization routes in Europe. Mol. Ecol. 7, 453–464.
Tajima, F., 1989. Statistical method for testing the neutral mutation hypothesis by DNA polymorphism. Genetics 123, 585–595.
Tarasov, P.E., Volkova, V.S., Webb III, T., Guiot, J., Andreev, A.A., Bezusko, L.G., Sevastyanov, D.V., 2000. Last glacial maximum biomes reconstructed from pollen and plant macrofossil data from northern Eurasia. J. Biogeogr. 27, 609–620.
Tyrberg, T., 1998. Pleistocene Birds of the Palearctic: A Catalogue. Nuttall Ornithological Club, Cambridge.
Van Andel, T.H., Tzedakis, P.C., 1996. Palaeolithic landscapes of Europe and environs, 150,000–25,000 years ago: an overview. Quatern Sci. Rev. 15, 481–500.
Van Meerbeeck, C.J., Renssen, H., Roche, D.M., 2009. How did Marine Isotope Stage 3 and Last Glacial Maximum climates differ? – perspectives from equilibrium simulations. Clim. Past. 5, 33–51.
Van Oosterhout, C., Hutchinson, W.F., Wills, D.P.M., Shipley, P., 2004. MICRO-CHECKER: For identifying and correcting genotyping errors in microsatellite data. Mol. Ecol. Notes 4, 535–538.
Veith, M., Schmidtler, J.F., Kosuch, J., Baran, I., Seitz, A., 2003. Palaeoclimatic changes explain Anatolian mountain frog evolution: a test for alternating vicariance and dispersal events. Mol. Ecol. 12, 185–199.
Villesen, P., 2007. FaBox: an online toolbox for fasta sequences. Mol. Ecol. Notes 7, 965–968. https://doi.org/10.1111/j.1471-8286.2007.01821.x.
Wagner, C.E., Keller, I., Wittwer, S., Selz, O.M., Mwaiko, S., Greuter, L., Sivasundar, A., Seehausen, O., 2012. Genome-wide RAD sequence data provide unprecedented resolution of species boundaries and relationships in the Lake Victoria cichlid adaptive radiation. Mol. Ecol. 22, 787–798.
Wenink, P.W., Baker, A.J., Rösner, H.-U., Tilanus, M.G.J., 1996. Global mitochondrial DNA phylogeography of Holarctic breeding Dunlis (*Calidris alpina*). Evolution 50, 318–330.
Willis, S.C., Macrander, J., Farias, I.P., Ortí, G., 2012. Simultaneous delimitation of species and quantification of interspecific hybridization in Amazonian peacock cichlids (genus *Cichla*) using multi-locus data. BMC Evol. Biol. 12, 96.
Wink, M., Seibold, I., Lotfikhah, F., Bednarek, W., 1998. Molecular systematics of holarctic raptors (Order Falconiforines). In: Chancellor, R.D., Meyburg, B.-.U., Ferrero, J.J. (Eds.), Holarctic Birds of Prey. Adenex-WWGBP, pp. 29–34.
Zink, R.M., 2004. The role of subspecies in obscuring avian biological diversity and misleading conservation policy. Proc. R. Soc. Lon. 271, 561–564.